INTERNATIONAL JOURNAL OF ENERGY RESEARCH
Int. J. Energy Res. 2000; **24**:151–161

An adaptive feedback linearization strategy for variable speed wind energy conversion systems

F. Valenciaga, P. F. Puleston*,†,‡, P. E. Battaiotto and R. J. Mantz‡

Laboratorio de Electrónica Industrial, Control e Instrumentación (LEICI), Departamento de Electrotecnia, Facultad de Ingeniería, Universidad Nacional de La Plata, CC91 (1900) La Plata, Argentina

SUMMARY

This paper presents a control strategy based on adaptive feedback linearization intended for variable speed grid-connected wind energy conversion systems (WECS). The proposed adaptive control law accomplishes energy capture maximization by tracking the wind speed fluctuations. In addition, it linearizes the system even in the presence of turbine model uncertainties, allowing the closed-loop dynamic behaviour to be determined by a simple tuning of the controller parameters. Particularly, the attention is focused on WECS with slip power recovery, which use a power conversion stage as a rotor-controlled double-output induction generator. However, the concepts behind the proposed control strategy are general and can be easily extended to other WECS configurations. Copyright © 2000 John Wiley & Sons, Ltd.

KEY WORDS: wind energy; adaptive control; feedback linearization

1. INTRODUCTION

The increasing rate of consumption of fossil and nuclear fuels has drawn worldwide interest to alternative energy technologies. Lately, wind power has been recognized as one of the few renewable energy sources that can offer pollution free electricity nearly cost competitive with conventional energy methods (Godoy Simoes *et al*., 1997).

It has been shown previously (Spée and Enslin, 1995; Novak *et al*., 1995) that, in grid connected applications, the efficiency of constant speed generation systems is smaller than that of variable speed systems. So, despite the extra cost of power electronics and control, the life-cycle cost is lower. With the improvement of power semiconductors and AC drives, many different configuration of variable speed WECS have been developed. Among them, one interesting option is given by the use of a slip power recovery drive. Typically, this system consist of a double output induction generator (DOIG) and a static Kramer Drive (SKD), namely: an uncontrolled bridge

* Correspondence to: P. F. Puleston, Laboratorio de Electrónica Industrial, Control e Instrumentación (LEICI), Departamento de Electrotecnia, Facultad de Ingeniería, Universidad Nacional de La Plata, CC91 (1900) La Plata, Argentina.
† e-mail: puleston@venus.fisica.unlp.edu.ar
‡ Professors R. J. Mantz and P. F. Puleston are also members of CICPBA and CONICET, respectively.

Received 16 February 1998
Accepted 7 May 1999

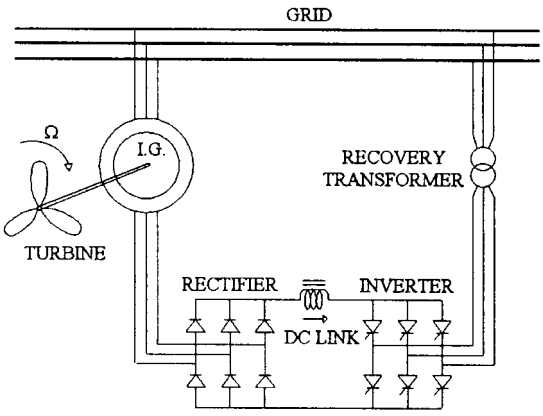

Figure 1. Schematic diagram of the WECS with DOIG.

rectifier, a line commutated inverter and a smoothing reactor (see Figure 1). In such configuration the stator power is directly fed to the grid while rotor power is partially recovered through the SKD. The generator torque, and hence the system speed, can be controlled by modifying the firing angle of the inverter (Ermis *et al*., 1992; Puleston, 1997).

In this paper an adaptive feedback linearization strategy for WECS with slip power recovery is presented. The main control objective is energy capture maximization by tracking the changes in wind speed and consequently maintaining optimum aerodynamic efficiency. Moreover, the proposed adaptive law allows system linearization even in the presence of an imprecise turbine description. Then, the closed-loop dynamic behaviour can be determined by a simple tuning of the controller parameters.

The outline of the paper is as follows. In Section 2 a brief description of the system and its mathematical model is given. Using this model, in Section 3, the proposed control strategy is developed and analysed. Section 4 presents the simulation results. Finally, conclusions are discussed in Section 5.

2. FUNDAMENTALS OF WECS WITH DOIG

The amount of wind converted into mechanical power by the turbine is given by (Smith, 1995)

$$P_t(v, \Omega) = \tfrac{1}{2} C_p(v, \Omega) \pi \rho r^2 v^3 \tag{1}$$

where ρ is the air density, r is the turbine radius, v is the wind speed and Ω is the shaft speed. The power coefficient C_p is the ratio of mechanical power delivered to total power of the captured wind. C_p is a non-linear function of v and Ω, and is highly dependent on the constructive characteristics of the turbine. Typically, it is given as a function of the tip speed ratio λ, that is the ratio of turbine speed at the tip of the blade to wind speed:

$$\lambda = r\Omega / v \tag{2}$$

A typical C_p characteristic is displayed in Figure 2. It can be observed that wind turbines are most efficient at one tip speed ratio ($\lambda = \lambda_{opt}$). So, to extract maximum power from the wind,

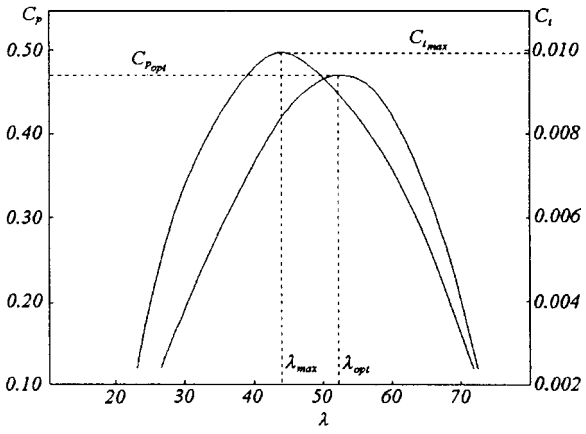

Figure 2. Power coefficient (C_p) and torque coefficient (C_t).

the control system should modify shaft speed in order to maintain $\lambda = \lambda_{opt}$ in spite of wind fluctuation.

The torque developed by the turbine can be obtained from Equation (1)

$$T_t(v, \Omega) = \frac{P_t(v, \Omega)}{\Omega} = \frac{1}{2} C_t(\lambda) \pi \rho r^3 v^2 \tag{3}$$

where $C_t(\lambda)$ is the torque coefficient of the turbine and is given by $C_t(\lambda) = C_p(\lambda)/\lambda$ (see Figure 2).

Figure 3 shows torque–shaft speed ($T - \Omega$) characteristics of a turbine, with wind speed as parameter. The operation points of maximum power transference are marked on each curve. It can be observed that they do not match with maximum torque points (see in Figure 2 that $\lambda_{max} \neq \lambda_{opt}$).

On the other hand, the torque of the electrical subsystem (DOIG with slip power recovery drive, shown in Figure 1) can be controlled through the firing angle α of the KDS. The equation of the generator torque as a function of α is given by (Puleston, 1997)

$$T_g = \frac{3 V_s^2 s R_{eq}}{\Omega_s [(s R_s + R_{eq})^2 + (s\omega_s L_{ls} + s\omega_s L_{lr})^2]} \tag{4}$$

where

$$R_{eq} = \frac{s[n_2^2 s R_b + (n_1 |\cos(\alpha)|)^2 R_s - n_1 |\cos(\alpha)| \sqrt{\Gamma}]}{((n_2 s)^2 - (n_1 |\cos(\alpha)|)^2)}$$

$$R_b = R_r + 0.55 R_f$$

$$\Gamma = 2 n_2^2 R_b s R_s + (n_2 s R_s)^2 + n_2^2 (s\omega_s L_{ls} + s\omega_s L_{lr})^2 + (n_2 R_b)^2 - [n_1 |\cos(\alpha)| (\omega_s L_{ls} + \omega_s L_{lr})]^2$$

s is the slip, V_s the grid phase voltage, n_1 the ratio of stator number of turns to rotor number of turns, n_2 the turns ratio of the output transformer, R_r, R_s, R_f the resistance of rotor, stator and

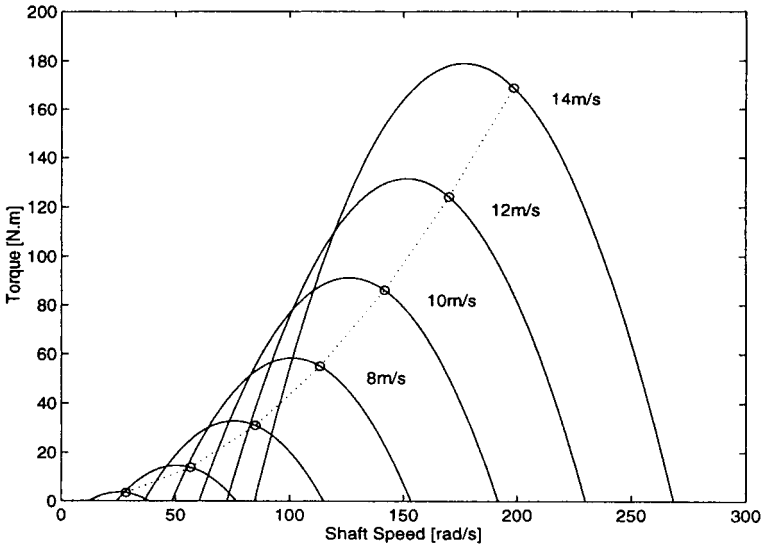

Figure 3. Torque versus shaft speed characteristics of a wind turbine (T_t-Ω) for different values of wind speed.

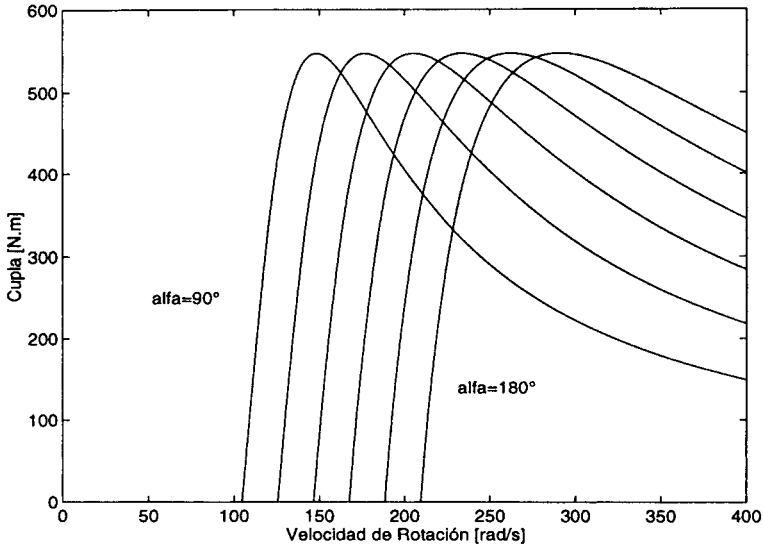

Figure 4. Torque versus shaft speed characteristics (T_g-Ω) of a GIDS-KDS for different values of α.

smoothing reactor, respectively, L_{ls} the leakage inductance of stator, L_{lr} the leakage inductance of rotor, α the firing angle of the inverter, ω_s the synchronous electrical angular frequency and Ω_s the synchronous rotational speed.

In Figure 4 torque T_g is plotted versus speed Ω for different values of the firing angle α. The expression of the generator torque (Equation (4)) can be simplified, for practical purposes, by

using a first-order approximation (Puleston, 1997)

$$T_g(\Omega, \alpha) = \frac{3V_s^2}{\Omega_s^2 R_b n_2}\Omega - \frac{3V_s^2(n_1|\cos(\alpha)| + n_2)}{\Omega_s R_b n_2} = H_0\Omega - H_1 u \tag{5}$$

where H_0, y, H_1 are positive constants and $u = 1 + (n_1/n_2)|\cos(\alpha)|$.

Finally, the dynamic behaviour of the WECS is described by the mechanical balance equation (Ermis *et al.*, 1992)

$$J\dot{\Omega} = T_t(v, \Omega) - T_g(\alpha, \Omega) \tag{6}$$

where the friction term has been neglected and J is the inertia of the rotating parts.

3. CONTROL STRATEGY

The primary control objective of the proposed strategy is energy capture maximization while setting the tracking error dynamic. However, the controller design for a highly non-linear system such as a WECS (see Equation (3)) can be extremely complicated. Such designing difficulties are overcome by using feedback linearization techniques. Furthermore, the development of an adaptive feedback linearization strategy is needed to deal with the frequent uncertainties in turbine characterization. So, the proposed strategy permits system linearization even in the presence of model uncertainty.

The first step to obtain the linearizing control law is rewriting Equation (6) in the form

$$\dot{\Omega} = \frac{T_t(v, \Omega)}{J} - \frac{H_0}{J}\Omega + \frac{H_1}{J}u \tag{7}$$

where the turbine torque T_t is the variable to whom adaptive estimation will be applied. Choosing the control law as

$$u = \frac{J}{H_1}\left(\frac{H_0}{J}\Omega - \frac{\hat{T}_t}{J} + \vartheta\right) \tag{8}$$

with $\hat{T}_t$ an estimate of T_t and ϑ an auxiliary control input. Substituting Equation (8) into Equation (7) provides

$$\dot{\Omega} = \frac{1}{J}(T_t - \hat{T}_t) + \vartheta = \frac{\tilde{T}_t}{J} + \vartheta \tag{9}$$

To maximize the energy conversion efficiency over a wide range of wind speeds, the rotational speed must track the reference law

$$\Omega_{ref} = \frac{\lambda_{opt} v}{r} \tag{10}$$

in order to operate at the point of maximum energy extraction (C_{Popt}). Then the tracking error is defined as

$$e = \Omega - \Omega_{ref} \tag{11}$$

Substituting Equation (9) into Equation (11) an differentiating, gives

$$\dot{e} = \dot{\Omega} - \dot{\Omega}_{\text{ref}} = \frac{1}{J}(T_{\text{t}} - \hat{T}_{\text{t}}) + \vartheta - \dot{\Omega}_{\text{ref}} \tag{12}$$

Now, if the auxiliary control input is selected, $\vartheta = \dot{\Omega}_{\text{ref}} - Ke$, and is substituted into Equation (12), the following results:

$$\dot{e} = -Ke + \frac{1}{J}(T_{\text{t}} - \hat{T}_{\text{t}}) = -Ke + \frac{1}{J}\tilde{T}_{\text{t}}$$

$$\dot{e} = Ae + B\tilde{T}_{\text{t}} \tag{13}$$

where K is a design parameter of the controller.

An adjustment law for the estimation, which guarantees closed-loop stability, can be obtained by proposing an adequate Lypunov function (Åström and Wittenmark, 1995; Slotine and Weiping, 1991). Given that the error Equation (13) is linear and matrix A is negative definite, is possible to find a positive-definite matrix P such that

$$A^{\text{T}}P + PA = -I \tag{14}$$

Then, an appropriate Lypunov function is

$$V = e^{\text{T}}Pe + \tilde{T}_{\text{t}}^2/\gamma \tag{15}$$

where the adaptation gain γ is another design parameter of the controller. Differentiating Equation (15) gives

$$\dot{V} = -e^{\text{T}}e + 2\tilde{T}_{\text{t}}B^{\text{T}}Pe + \frac{2}{\gamma}\tilde{T}_{\text{t}}\dot{T}_{\text{t}} - \frac{2}{\gamma}\tilde{T}_{\text{t}}\dot{\hat{T}}_{t} \tag{16}$$

To guarantee asymptotic convergence $\dot{V}$ must be negative definite. In order to assure this, the second and fourth terms of Equation (16) can be cancelled by choosing the following adjustment law for the estimate $\hat{T}_{\text{t}}$:

$$\dot{\hat{T}}_{\text{t}} = \frac{\gamma e}{2KJ} \tag{17}$$

Then, Equation (16) becomes

$$\dot{V} = -e^{\text{T}}e + \frac{2}{\gamma}\tilde{T}_{\text{t}}\dot{T}_{\text{t}} \tag{18}$$

Even though the first term of Equation (18) is always negative, nothing is said about the sign of the second term. However, if product $\tilde{T}_{\text{t}}\dot{T}_{\text{t}}$ is bounded such that

$$e^{\text{T}}e > \frac{2}{\gamma}|\tilde{T}_{\text{t}}\dot{T}_{\text{t}}|_{\max} \tag{19}$$

convergence can be guaranteed in the region of the $e - \tilde{T}_{\text{t}}$ plane wherein Equation (19) is verified.

To find an upper bound for $\tilde{T}_{\text{t}}\dot{T}_{\text{t}}$ implies to find bounds for each factor $\tilde{T}_{\text{t}}$ and $\dot{T}_{\text{t}}$. These bounds can be determined by knowing:

(a) the extreme values of the shaft speed;
(b) the extreme values of the wind speed;
(c) the maximum rate of variation of the shaft speed;
(d) the maximum rate of variation of the wind speed and
(e) bounds for $C_{\text{t}}(\lambda)$ uncertainty.

The values cited in (a) and (b) are established according to the operation range of the WECS. Point (c) is determined by the desired closed-loop dynamic behaviour of the system, while point (d) is inferred from the analysis of wind data from the site. Finally, the bounds in point (e) are computed from the available information of the turbine.

The equations of $\tilde{T}_t$ and $\dot{T}_t$ are obtained from Equations (13) and (3), respectively:

$$\tilde{T}_t = J\dot{\Omega} - J\dot{\Omega}_{ref} + K\Omega - K\Omega_{ref} \tag{20}$$

$$\dot{T}_t = \frac{1}{2}\pi\rho r^3 \left[rv\dot{\Omega}\frac{C_t(\lambda)}{d\lambda} - r\Omega\dot{v}\frac{C_t(\lambda)}{d\lambda} + C_t(\lambda)2v\dot{v} \right] \tag{21}$$

These equations can be bounded and written as

$$|\dot{T}_t|_{max} \leqslant M_1, \quad |\tilde{T}_t|_{max} \leqslant M_2 + M_3 K \tag{22}$$

where M_1, M_2 and M_3 are positive bounds determined from the information summarized in points (a)–(e). Conservative expressions for them are given by

$$M_1 = \frac{1}{2}\pi\rho r^3 \left[rv_{max}\dot{\Omega}_{max}\frac{C_t}{d\lambda}\bigg|_{max} + r\Omega_{max}\dot{v}_{max}\frac{C_t}{d\lambda}\bigg|_{max} + C_{t\,max}\,2v_{max}\dot{v}_{max} \right] \tag{23}$$

$$M_2 = J\left[\dot{\Omega}_{max} + \frac{\lambda_{opt}}{r}\dot{v}_{max} \right] \tag{24}$$

$$M_3 = \Omega_{max} - \Omega_s \tag{25}$$

Substituting Equation (22) into Equation (19) results:

$$e^T e > \frac{2}{\gamma}(M_1 M_2 + M_1 M_3 K) \tag{26}$$

In addition, the transfer functions of the resulting linear system are obtained from Equations (13) and (17)

$$\frac{e}{T_t} = \frac{S/J}{S^2 + KS + \gamma/2KJ^2} \tag{27}$$

$$\frac{\hat{T}_t}{T_t} = \frac{\gamma/2KJ^2}{S^2 + KS + \gamma/2KJ^2} \tag{28}$$

The latter expressions, together with Equation (26), show the existence of a trade off between the desired dynamic behaviour and the size of the convergence region. So, it is clear that the control parameters (K and γ) must be chosen by means of Equations (26)–(28), taken both aspects into consideration.

4. SIMULATION RESULTS

Simulation results of the proposed strategy controlling a 30 kW horizontal axis WECS with DOIG are presented in this section. The generator is connected to a 220 V–50 Hz grid, the inertia of the rotating parts (high-speed side) is 3.9 kg m^{-2} and the λ_{opt} of the turbine is 51.

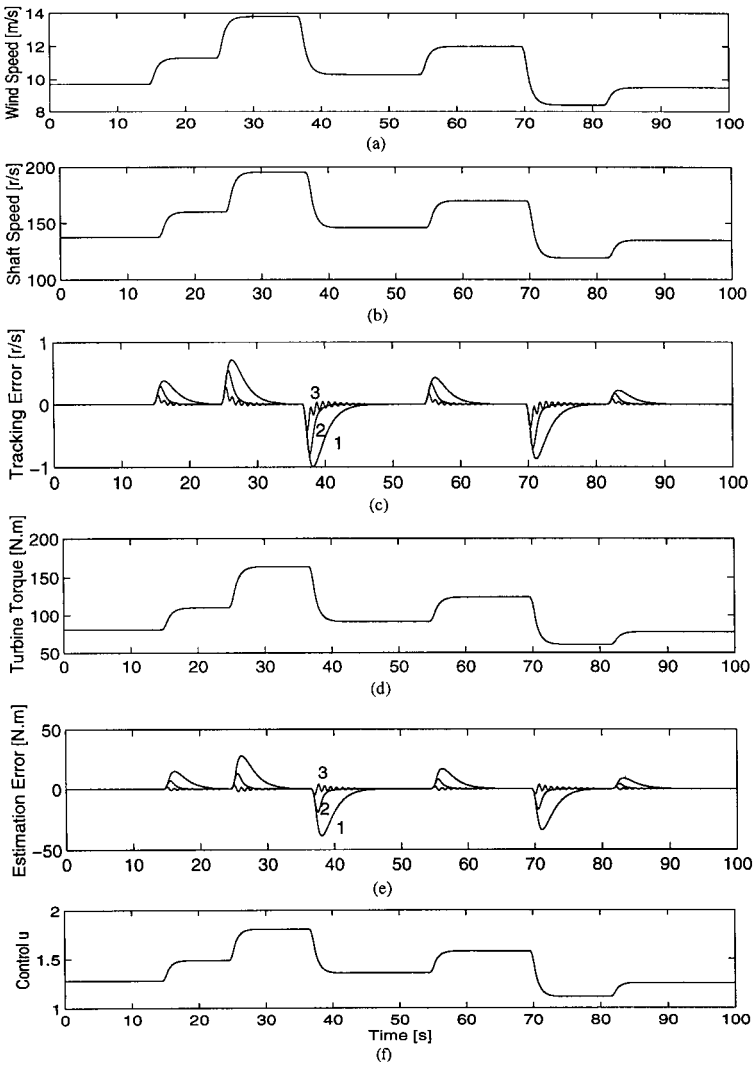

Figure 5. Time evolution of the system variables. (a) Wind speed v. (b) Shaft speed Ω. (c) Tracking error e. Curve 1: $p_1 = -9.36$ and $p_2 = -0.36$. Curve 2: $p_1 = -2.9 + \mathrm{j}2.9$ and $p_2 = -2.9 - \mathrm{j}2.9$. Curve 3: $p_1 = -0.3 + \mathrm{j}7$ and $p_2 = -0.3 - \mathrm{j}7$. (d) Turbine torque T_t. (e) Estimation error $\tilde{T}_\mathrm{t}$. (f) Control action u.

The wind speed profile used for the simulation is depicted in Figure 5(a). Even though real wind does not occur as a series of filtered steps, this time series has been used because it is a standard testing signal that permits a clear interpretation of the system behaviour.

In Figures 5(b) and 5(d) the evolution of the shaft speed and the turbine torque are plotted. The variation of shaft speed follow the variation of wind speed in order to operate at constant $\lambda = \lambda_{\mathrm{opt}}$.

In correspondence with Figures 5(b) and 5(d), Figures 5(c) and 5(e) show the tracking error e and the estimation error $\tilde{T}_\mathrm{t}$ for different values of the controller parameters. In curve (1) $K = 10$

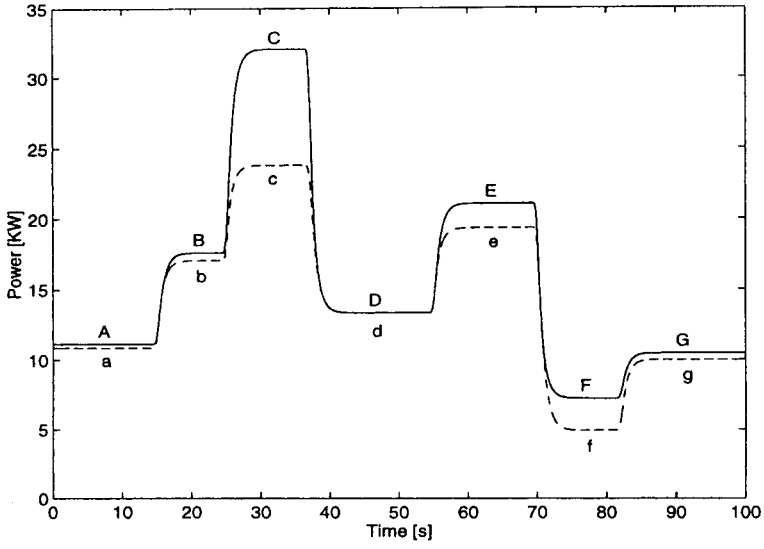

Figure 6. Wind power captured. Variable speed WECS controlled by the proposed strategy (solid line). Fixed speed WECS (dashed line).

and $\gamma = 1800$, in curve (2) $K = 5.28$ and $\gamma = 3060$ and in curve (3) $K = 0.6$ and $\gamma = 900$. The closed-loop poles given by Equations (27) and (28) are, respectively, placed in: (1) $p_1 = -9.36$ and $p_2 = -0.36$, (2) $p_1 = -2.9 + j2.9$ and $p_2 = 2.9 - j2.9$ and (3) $p_1 = -0.3 + j7$ and $p_2 = -0.3 - j7$. It can be observed that the closed-loop error responses go from overdamped to oscillatory as they were specified in the design. The evolution of control action u is displayed in Figure 5(f).

To assess the effectiveness of the proposed strategy controlling a variable speed WECS, the wind power captured by the system under consideration is compared to that of a WECS with cage induction generator directly connected to the grid. The latter is the most widespread architecture among fixed speed wind turbines. Figure 6 shows that the power captured by the variable speed WECS always surpasses (or at least equates) that of the fixed speed WECS. The aerodynamic efficiencies of both systems only match during the interval $42s < t < 54s$. The reason is that a fixed speed system is capable to maintain $\lambda = \lambda_{opt}$ at only one wind speed. For this particular case it was designed for $v = 10.5\,\mathrm{m\,s^{-1}}$.

A presentation in the torque versus shaft speed plane may help to clarify this concept (Figure 7). The torque-speed characteristics (for different wind speeds) and the points of maximum aerodynamic efficiency are plotted in dotted and dashed lines, respectively. In Figure 7(a) the DOIG torque characteristics (for different values of the firing angle) are represented in dot and dash, while the evolution of the turbine torque of the variable speed WECS is in solid line. In the same manner, Figure 7(b) presents the cage induction generator torque characteristic and the evolution of the turbine torque of the fixed speed WECS.

Operation points A–G and a–g are in correspondence with the steady-state intervals indicated in Figure 6. It can be observed that the proposed controller makes the system move over the

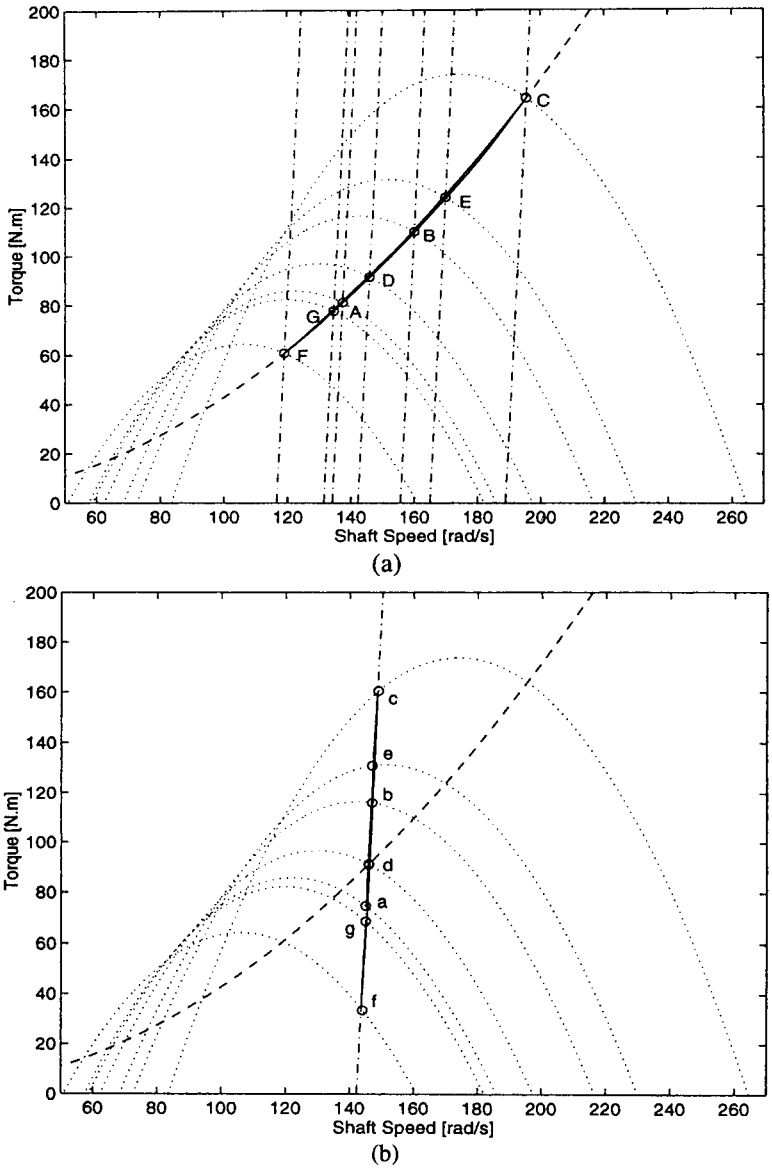

Figure 7. Torque versus shaft speed representation. Torque-speed characteristics for different wind speeds (dotted lines). Maximum aerodynamic efficiency locus (dashed line). (a) DOIG torque characteristics for different values of the firing angle (dotted and dashed lines) and turbine torque evolution of the variable speed WECS (solid line). (b) Cage induction generator torque characteristic (dotted and dashed lines) and evolution of the turbine torque of the fixed speed WECS (solid line).

maximum efficiency locus. On the other hand, the fixed speed system shifts over the cage induction generator characteristic, being able to intersect the maximum efficiency locus only at point d.

5. CONCLUSIONS

A control strategy to optimize power generation of variable speed grid-connected WECS was presented. The proposed controller is based on feedback linearization theory in order to deal with a system of highly non-linear characteristics. Adaptive features were required to enable the feedback law to linearize the system even while facing uncertainties in the turbine description. Consequently, the dynamics of the tracking error and the turbine torque estimation error can be easily assigned by tuning two control parameters (K and γ).

However, it is demonstrated that the region where convergence is guaranteed also depends on these parameters. An expression establishing this relationship is provided. Through it, the trade off between the desired dynamics and the size of the convergence region can be taken into consideration in the design procedure.

The effectiveness of the control has been demonstrated through the use of computer simulation. The improvements in energy conversion efficiency have been shown comparing the energy captured by the system under consideration to that of a WECS with cage induction generator directly connected to grid (the most widespread architecture among fixed speed wind turbines).

Finally, it is important to remark that even though calculations were made for a particular variable speed WECS, the ideas behind the control strategy developed in this paper are general and can be readily extended to other variable speed wind energy conversion topologies.

REFERENCES

Akpinar E, Trahan RE, Nguyen AD. 1993 Modeling and analysis of closed-loop slip energy recovery induction motor drive using a linearization technique. *IEEE Transactions on Energy Conversion* **8**(4):688–696.

Åström K, Wittenmark B. 1995. *Adaptive Control*. Addison-Wesley: Reading MA.

Ermis M *et al*. 1992. Various induction generator schemes for wind electricity generation. *Electric Power Systems Research* **23**:71–83.

Godoy Simoes M, Bose BK, Spiegel RJ. 1997. Fuzzy logic based intelligent control of a variable speed cage machine wind generation system. *IEEE Transactions on Power Electronics* **2**(1):87–95.

Novak P, Ekelund T, Jovik Y, Schmidtbauer B. 1995. Modeling and control of variable-speed wind-turbine drive system dynamics. *IEEE Control Systems Magazine* **15**:28–37.

Puleston PF. 1997. Control of WECS with double output induction generator. *Ph.D. Thesis*, EE Department, National University of La Plata, Argentina.

Slotine JJ, Weiping Li. 1991. *Applied Nonlineal Control*. Prentice-Hall: Englewood Cliffs, NJ.

Smith GA. 1995. Power electronics for recovery of wind and solar energy. *Wind Engineering* **19**(2):53–66.

Spée R, Enslin JH. 1995. Novel control strategies for variable-speed doubly fed wind power generation systems. *Renewable Energy* **6**(8):907–915.

